

5-28-2001

Phonon-pumped terahertz gain in n-type GaAs/ AlGaAs superlattices

Greg Sun

University of Massachusetts Boston, greg.sun@umb.edu

Richard A. Soref

Air Force Research Laboratory, Hanscom Air Force Base

Follow this and additional works at: http://scholarworks.umb.edu/physics_faculty_pubs



Part of the [Physics Commons](#)

Recommended Citation

Sun, Greg and Soref, Richard A., "Phonon-pumped terahertz gain in n-type GaAs/AlGaAs superlattices" (2001). *Physics Faculty Publications*. Paper 26.

http://scholarworks.umb.edu/physics_faculty_pubs/26

This Article is brought to you for free and open access by the Physics at ScholarWorks at UMass Boston. It has been accepted for inclusion in Physics Faculty Publications by an authorized administrator of ScholarWorks at UMass Boston. For more information, please contact libraryuasc@umb.edu.

Phonon-pumped terahertz gain in n-type GaAs/AlGaAs superlattices

Gregory Sun and Richard A. Soref

Citation: *Appl. Phys. Lett.* **78**, 3520 (2001); doi: 10.1063/1.1376432

View online: <http://dx.doi.org/10.1063/1.1376432>

View Table of Contents: <http://apl.aip.org/resource/1/APPLAB/v78/i22>

Published by the [American Institute of Physics](#).

Related Articles

Electroluminescence from strained germanium membranes and implications for an efficient Si-compatible laser
Appl. Phys. Lett. **100**, 131112 (2012)

A weakly coupled semiconductor superlattice as a potential for a radio frequency modulated terahertz light emitter
Appl. Phys. Lett. **100**, 131104 (2012)

Quantum-dot nano-cavity lasers with Purcell-enhanced stimulated emission
Appl. Phys. Lett. **100**, 131107 (2012)

Effect of internal optical loss on the modulation bandwidth of a quantum dot laser
Appl. Phys. Lett. **100**, 131106 (2012)

Design of three-well indirect pumping terahertz quantum cascade lasers for high optical gain based on nonequilibrium Green's function analysis
Appl. Phys. Lett. **100**, 122110 (2012)

Additional information on *Appl. Phys. Lett.*

Journal Homepage: <http://apl.aip.org/>

Journal Information: http://apl.aip.org/about/about_the_journal

Top downloads: http://apl.aip.org/features/most_downloaded

Information for Authors: <http://apl.aip.org/authors>

ADVERTISEMENT



ACCELERATE AMBER AND NAMD BY 5X.
TRY IT ON A FREE, REMOTELY-HOSTED CLUSTER.

LEARN MORE

Phonon-pumped terahertz gain in *n*-type GaAs/AlGaAs superlattices

Gregory Sun^{a)}

Department of Physics, University of Massachusetts at Boston, Boston, Massachusetts 02125

Richard A. Soref

Sensors Directorate, Air Force Research Laboratory, Hanscom Air Force Base, Massachusetts 01731

(Received 2 February 2001; accepted for publication 10 April 2001)

Local population inversion and far-IR gain are proposed and theoretically analyzed for an unbiased *n*-doped GaAs/Al_{0.15}Ga_{0.85}As superlattice pumped solely by phonons. The lasing transition occurs at the Brillouin zone boundary of the superlattice wave vector k_z between the two conduction minibands CB1 and CB2 of the opposite curvature in k_z space. The proposed waveguided structure is contacted above and below by heat sinks at 300 K and 77 K, respectively. Atop the superlattice, a heat buffer layer confines longitudinal optical phonons for enhanced optical-phonon pumping of CB1 electrons. A gain of 345 cm^{-1} at 4.5 THz is predicted for a doping density of $2.8 \times 10^{16} \text{ cm}^{-3}$. © 2001 American Institute of Physics. [DOI: 10.1063/1.1376432]

The phonon-pumped laser (PPL) is a radical kind of semiconductor interminiband laser that uses a temperature gradient and optical phonons to excite carriers from the ground-state miniband of a superlattice to an excited miniband. The PPL does not utilize optical pumping or electrical pumping; it has no electrical contacts and operates under the flat-band condition. In a recent manuscript,¹ we proposed a PPL design for the valence minibands of a SiGe/Si superlattice. In this letter, we propose and analyze phonon pumping of a *n*-doped GaAs/AlGaAs superlattice. We show, via calculations, that significant gain appears feasible at THz frequencies—gain that is potentially sufficient for lasing.

Figures 1 and 2 show, respectively, the cross sectional end view and the perspective view of our proposed GaAs THz PPL. The device structure is an edge-emitting metal-coated surface-plasmon strip waveguide that is sandwiched between a warm heat sink at temperature T_2 and a cool heat sink at temperature T_1 . The sinks contact the upper and lower gold claddings of the waveguide. The waveguide supports a single transverse magnetic (TM)₀-like mode and has cleaved ends to form a Fabry–Perot resonator. Referring to Fig. 1, the undercoated substrate is (100) GaAs. On it, a buffer layer of undoped GaAs is grown in order to increase the waveguide thickness to several micrometers if the epitaxy machine limits the superlattice (SL) stack height to $\sim 1 \mu\text{m}$. Next, a ~ 100 period *n*-doped GaAs/Al_{1-x}Ga_xAs superlattice is grown, followed by growth of a second undoped GaAs waveguide spacer layer. Then a heat buffer layer (HBL) is deposited on the structure, followed by deposition of a metal film. Optic and acoustic phonons are launched from the GaAs substrate and travel upward through the SL towards the HBL. The HBL material is chosen so that its optical phonon spectra are different from those of the SL. Consequently, as optical phonons reach the HBL interface, the discontinuity in spectra causes optical phonons to be reflected back down to the SL, thereby confining those phonons in the waveguide; whereas the up-traveling acoustic phonons penetrate through the HBL and are lost. For the

present materials system, we believe that an AlAs layer will act as an adequate HBL.

The inset in Fig. 1 shows the effective temperatures of optical and acoustic phonons, T_0 and T_a respectively, as a function of z . Using heat-diffusion equations, a detailed analysis¹ shows that T_0 is maintained nearly equal to T_2 across the device structure up to the HBL as shown in Fig. 1. However, T_a drops steadily from T_2 down to T_1 across the structure. The SL is located closer to the T_1 end, as shown. There, a large difference in effective temperatures T_0 and T_a exists. This provides effective pumping of the ground-state electrons of the SL by longitudinal optical (LO) phonons. The next step in obtaining a THz laser is to use quantum engineering to design a SL that has, in effect, four levels in its dispersion diagram as well as a large radiative dipole matrix element $\langle u|z|l \rangle$ between the two minibands CB1 and CB2. For CB2-to-CB1 radiation, the z polarization is allowed and the xy polarization is forbidden.

The SL is a simple, square-well SL operating in the flat band condition. The quantum well and barrier widths (l_w and l_b , respectively) and the well and barrier Al compositions (x_w and x_b , respectively) are chosen so that the spacing between the first two minibands at zone center $E_2(k_z=0) - E_1(k_z=0) = E_{21}(0)$ is slightly less than the optical phonon energy $\hbar\omega_{\text{LO}}$ of GaAs (36.2 meV), to facilitate the CB1-to-

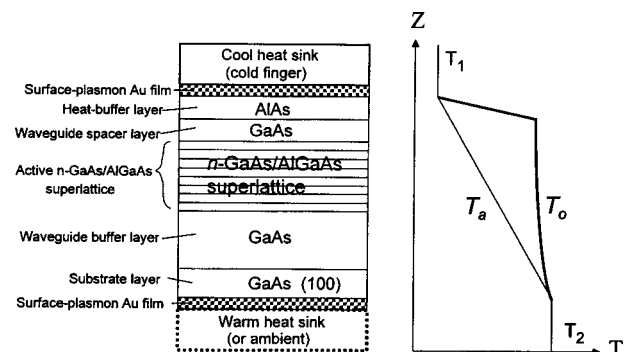


FIG. 1. End view of proposed phonon-pumped laser. Inset shows the effective-temperature distributions of acoustic and optical phonons.

^{a)}Electronic mail: gsun@cs.umb.edu

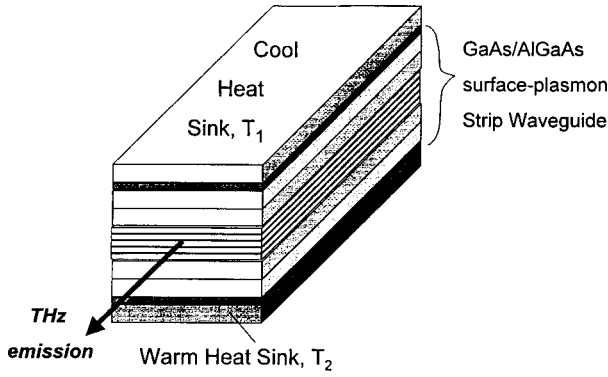


FIG. 2. Perspective view of the Fig. 1 laser.

CB2 optical-phonon pumping process and simultaneously to suppress the optical-phonon assisted CB2-to-CB1 relaxation process given the opposed dispersions for CB2 and CB1 as a function of the SL wave vector k_z . We also choose $l_w \gg l_b$ to give large matrix element $\langle u|z|l \rangle$. Using the $\mathbf{k} \cdot \mathbf{p}$ finite-element software from QSA Inc., we found (setting $x_w = 1$) that there is a range of x_b , l_w , and l_b that produces useful dispersion diagrams. A representative result is given in Fig. 3 for the SL of 210 Å GaAs QWs and 25 Å $\text{Al}_{0.15}\text{Ga}_{0.85}\text{As}$ barriers. The CB electron energy is cited with reference to the top of the HH valence band. The energy minimum of CB1 lies at the SL Brillouin zone center, while the minimum of CB2 occurs at the zone boundary $k_z = \pi/L$, where $L = l_w + l_b$ is the SL period. The choice of a wide GaAs quantum well in the SL produces a large dipole matrix element of 45 Å. Within each miniband, energy relaxation occurs mainly via interaction with acoustic phonons (plus some electron-electron scattering at higher densities). Since $\hbar\omega_{\text{LO}} \sim E_{21}(0)$, the population distribution between CB1 and CB2 is determined by the carrier-optical-phonon interaction.¹ We expect that the intraminiband scattering is faster than the interminiband process. As long as that is true, the distribution of carriers within each miniband is characterized by the acoustic phonon temperature T_a , while the distribution between minibands is governed by the optical phonon temperature T_0 . Disregarding the variation in the density of states, we have the total population of electrons N (provided by doping) distributed between the two minibands as

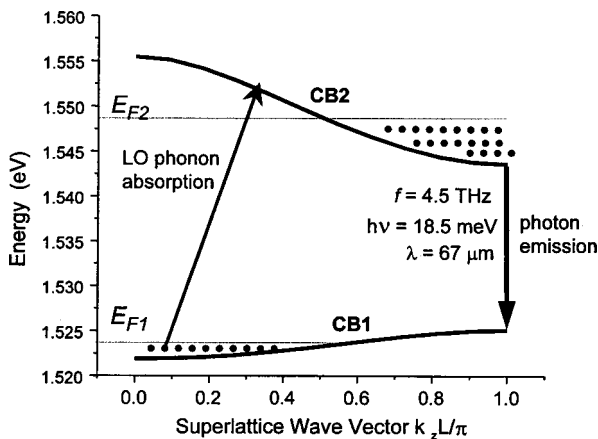


FIG. 3. Energy of the first two conduction minibands vs k_z . Quasi-Fermi levels for the n -doped ground miniband (E_{F1}) and the excited phonon-pumped miniband (E_{F2}) are shown.

$$N = N_1(E_{F1}, T_a) + N_2(E_{F2}, T_a), \quad (1)$$

where the population for CB2 (N_2) is related to that of CB1 (N_1) by

$$N_2 = N_1 \exp(-E_{21}/k_B T_0), \quad (2)$$

where k_B is the Boltzmann constant. The population distribution within each miniband is further characterized by quasi-Fermi levels E_{F1} and E_{F2} shown in Fig. 3, and by T_a , assuming quasi-equilibrium is established within CB2 and CB1 due to the fast intra-miniband process

$$N_i(E_{Fi}, T_a) = \frac{L}{\pi} \int_0^{\pi/L} dk_z \int_{E_i(k_z)}^{\infty} D(E) f(E, E_{Fi}, T_a) dE, \quad (3)$$

where $i = 1, 2$ for CB1 and CB2, respectively, $E_i(k_z)$ is the miniband energy dispersion as a function of SL wave vector k_z , and $D(E)$ is the density of states under the approximation of parabolic in-plane dispersion with effective mass m^* ,

$$D(E) = \frac{m^*}{\pi \hbar^2 L}, \quad (4)$$

and the Fermi-Dirac distribution is

$$f(E, E_{Fi}, T_a) = \frac{1}{1 + \exp(E - E_{Fi})/k_B T_a}. \quad (5)$$

Due to the upward slope of CB1 and the downward slope of CB2 in Fig. 3, it is possible to achieve local-in- k_z population inversion near the Brillouin zone boundary, even though N_2 is always less than N_1 . Absorption of optical phonons—the pumping process—is shown in Fig. 3 together with the vertical lasing transition at zone edge. The lower laser state at zone edge is rapidly emptied.

The energy of the lasing transition ($\hbar\omega_L$) in Fig. 3 is 18.5 meV corresponding to a 67 μm wavelength. The optical gain at this wavelength can be calculated as²

$$\gamma = \frac{2e^2 |\langle l|z|u \rangle|^2}{n \epsilon_0 (\hbar\Gamma)} \frac{2\pi}{\lambda_0} (N_u - N_l), \quad (6)$$

where e is the electronic charge, $(N_u - N_l)$ is the population difference between the upper and lower laser states, n is the refractive index of the SL, ϵ_0 is the permittivity of free space, $\hbar\Gamma$ is the full width at half maximum linewidth of the lasing line, and λ_0 is the free space wavelength. Our calculations indicate that $\langle u|z|l \rangle$ is 45 Å and we estimate that $\hbar\Gamma$ is 1 meV. Then, with the aid of Eqs. (1)–(6), we predict the 4.5 THz gain as a function of N . Our result is shown in Fig. 4 for the temperatures T_0 and T_a maintained at 300 K and 77 K, respectively. The gain is positive for a wide range of N , and the peak gain of $\gamma = 345 \text{ cm}^{-1}$ is obtained at a doping density of $2.8 \times 10^{16} \text{ cm}^{-3}$. Keeping T_0 at 300 K, preliminary estimates indicate that the gain in Fig. 4 decreases monotonically as T_a is increased from 77 to 150 K.

We wish to point out that, in addition to CB lasers, there are two practical possibilities for valence subband PPLs. The first approach is to “engineer” an inverted effective mass for the LH1 miniband as a function of in-plane wave vector k_x or k_y . As described earlier,^{3,4} this is done via a HH2–LH1 repulsion. Then, the PPL is obtained by making $E(\text{LH}1, 0) - E(\text{HH}1, 0) \sim \hbar\omega_{\text{LO}}$. This PPL would be a VCSEL since

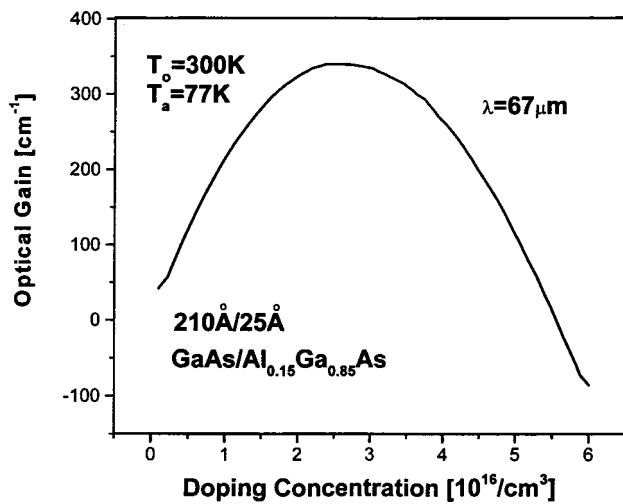


FIG. 4. Calculated optical gain for the Fig. 1 device as a function of doping density.

the allowed LH1–HH1 transition is xy polarized. Here, multilayer dielectric mirrors would replace the plasmon layers and the cool heat sink would be transparent to the surface-normal THz emission. The second possibility is a HH2–HH1 PPL, as discussed for SiGe/Si.¹ Here, HH2 and HH1 curve towards each other versus k_2 as desired, although the intervening LH1 curve runs parallel to HH1. In that case, the LH1–HH1 radiative interaction is negligible because the TM-polarized cavity selects HH2–HH1.

The valence-or-conduction miniband PPL principle applies to a variety of IV–IV, III–V, and II–VI semiconduc-

tors that have either zincblende or wurtzite lattices. We have estimated the photon energy, $\hbar\omega_L$, for a few examples of PPL semiconductor SL systems that have $E_{21}(0) \sim 0.95\hbar\omega_{LO}$ and $\hbar\omega_L \sim 0.60\hbar\omega_{LO}$. We choose a quantum well composition that is close to the barrier composition so that the well depth is roughly $2\hbar\omega_{LO}$. From the semiconductor literature, it is found that the LO optical phonon energy at 300 K is 110.1 meV for AlN (wurtz), 42.2 meV for AlSb (zb), and 43.6 meV for ZnS (zb). Then, we predict the following PPL radiative energies ($\hbar\omega_L$): 66 meV for $\text{Al}_{1-x}\text{Ga}_x\text{N}/\text{AlN}$, 25 meV for $\text{Al}_{1-x}\text{Ga}_x\text{Sb}/\text{AlSb}$, and 26 meV for $\text{ZnS}_{1-x}\text{Se}_x/\text{ZnS}$.

In conclusion, we have theoretically investigated the possibility of local-in- k_z population inversion and THz gain in an unbiased flat-band GaAs/AlGaAs SL pumped by phonons only. A lateral temperature gradient is created across the SL using warm and cool heat sinks that contact the structure. An AlAs heat buffer layer reflects optical phonons back into the SL, making $T_0 > T_a$ for interminiband pumping by phonons. At $T_0 = 300$ K and $T_a = 77$ K, a gain of 345 cm^{-1} at 4.5 THz is predicted for 210 Å/25 Å GaAs/Al_{0.15}Ga_{0.85}As at $2.8 \times 10^{16}\text{ cm}^{-3}$ n -type doping. The PPL principle applies to a variety of IV–IV, III–V, and II–VI semiconductors.

¹G. Sun, R. A. Soref, and J. B. Khurgin, IEEE J. Sel. Top. Quantum Electron. (to be published).

²G. Sun and J. B. Khurgin, IEEE J. Quantum Electron. **29**, 1104 (1993).

³L. Friedman, G. Sun, and R. A. Soref, Appl. Phys. Lett. **78**, 401 (2001).

⁴R. A. Soref, L. Friedman, G. Sun, M. J. Noble, and L. R. Ram-Mohan, Proc. SPIE **3795**, 516 (1999).